HEAT TRANSFER AUGMENTATION IN THREE SIDES DIMPLE ROUGHENED SOLAR DUCT

[1]Dr. S. Gunasekhran, [2]Dr. K. Prabhu, [3]Mr. Suresh Babu, [4]Mr. Siddappa Nyamagoud,
[1] Professor, Dept. of Mechanical Engineering, Malla Reddy College of Engineering, Sec-100
[2]Associate Professor,Department of Mechanical Engineering, Malla Reddy College of Engineering, Sec-100
[3]Asst. Professor, Department of Mechanical Engineering, Malla Reddy College of Engineering, Sec-100
[4]Asst. Professor, Department of Mechanical Engineering, Malla Reddy College of Engineering, Sec-100

Abstract— The present paper deals with the experimental results of heat transfer, friction factor and thermal efficiency of a novel type of three sides concave dimple roughened solar air heater under fully developed turbulent flow conditions. Three sides concave dimple roughened solar air heaters have higher values of heat transfer than those of one side concave dimple roughened solar air heaters in the range of 25-86% for varying relative roughness pitch and 21-81% for varying relative roughness height for the same values of operating parameters. The rise in friction factor of three sides roughened duct over one side roughened duct for varying relative roughness pitch and relative roughness height was found to be respectively as 11-34% and 15-41%. The maximum values of Nusselts number is obtained at relative roughness pitch of 12 and relative roughness height of 0.036. The maximum values of friction factor is obtained at relative roughness pitch of 8 and relative roughness height of 0.045.

Keywords: Solar air heater, Dimple shape, One side roughened duct, Relative roughness pitch, Relative roughness height, Three sides roughened duct.

1. Introduction

Solar air heaters follow a solar thermal technology in which the energy from the sun is captured by an absorbing medium and used to heat air. Solar air heating is a renewable energy heating technology used to heat or condition air for buildings or process heat applications. It is typically the most cost-effective out of all the solar technologies, especially in commercial and industrial applications, and it addresses the largest usage of building energy in heating climates as space heating and industrial process heating [1]. The value of heat transfer coefficient and heat capacity for air is low which reduces the heat transfer rate and thus increases the heat loss to the surroundings. Efforts have been made to improve the thermal efficiency by devising roughness in the form of wires, ribs, dimples baffles, fins, making the surface corrugated and packed bed and many more [2]. The low efficiency of SAH is due to less heat transfer between the collector and beneath flowing air, consequently raising collector's temperature, which leads in greater heat loss from the collector's surface to the nearby surroundings [3-7]. Literature of SAH reveals that the development of laminar sub-layer on heat exchanging surfaces and low heat capacity of air are responsible for less heat transfer resulting in lower thermal efficiency [8-9]. Even though the implication of roughness on heat exchanging surfaces results in an appreciable enhancement in heat transfer from the collector's surface to the under flowing air, the increase in frictional losses needs to be considered precisely. Heat transfer augmentation must be achieved at the cost of minimizing frictional losses. In order to dismantle the viscous sub-layer the core flow mustn't be disturbed. This is the reason the selection of roughness geometry and orientation

is given utmost importance [10-14]. Prasad and Saini [9] provided roughness as transverse ribs of small height and explained the effects of p/e and e/Dh on heat transfer and friction factor. It was found that the maximum augmentation in Nu and f were 2.38 and 4.25 times respectively over the non roughened surface. Gupta et al. [15-16] studied the effect of, p/e, e/Dh, α and Re on the performance of an inclined wire roughened SAH and found that the maximum augmentation in Nu and f were at 60˚ angle of attack. Gupta et al also stated that in comparison to transverse wire, the inclined wire have more heat transfer augmentation due to development of the secondary flow accompanied with the destruction of the viscous sub-layer in the vicinity of the ribs attached to the roughened duct. Momin et al. [17] conducted experiments on V-shaped roughened ducts and discussed its effect on heat transfer and friction factor characteristics under a varying range of roughness geometries and flow parameters as Re between 2500-18000, e/Dh between 0.02-0.034 and constant p/e of 10. The maximum increase in Nusselts number and friction factor was found to be 2.30 and 2.83 times over non-roughened ducts. Varun et al. [18] provided roughness in the form of combination of transverse and inclined ribs and concluded that the geometry having p/e = 8 yielded maximum thermal efficiency.

There was a conclusive information in the literature that most of the roughness provided was limited to a single side (flow facing side) of the absorber plate. If roughness is provided to the side walls (2 nos) as well, they can participate in the heat transfer augmentation process accompanied by the slightest increase in pressure drop resulting in an appreciable enhancement in heat transfer [19-20]. The main objective of the present study is to provide roughness on the three sides (one top and two side walls) of the roughened duct and determine the augmentation in heat transfer and friction factor in compared to the single side roughened duct.

In the present investigation, roughness provided is in the form of concave dimple-shape on three sides and one side roughened duct under identical flow and geometrical conditions. The present paper projects the augmentation in Nusselts number and friction factor for three sides over one side roughened duct as a function of Reynolds number (Re), relative roughness pitch (p/e) and relative roughness height (e/Dh).

2. Experimental set-up and methodology

Experimentation under actual outdoor conditions has been performed on multiple sets of one and three sides roughened ducts containing dimple roughened absorber plates of varying roughness dimensions. The schematic diagram of the test setup is shown in Fig. 1. A 2130 mm x 630 mm wooden board of 25 mm thickness is used to formulate three ducts namely A, B and C. Each duct has a length of 2130 mm in which 630 mm serves as entry section and 1500 mm serves as test section. The entire duct design is based on ASHRAE Standard [21].

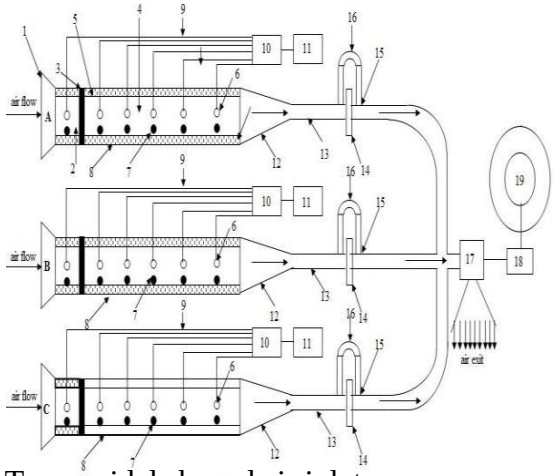

1. Trapezoidal shaped air inlet
2. Non-roughened duct section
3. Insulation between entry and test length
4. Insulation
5. Thermocouple
6. Thermometer
7. Glass covers
8. Copper wire
9. Selector switch
10. Digital voltmeter
11. Diverging section
12. Cylindrical pipe
13. Roughened duct section
14. Orifice-plate
15. Flange couplings
16. U-tube manometer
17. Blower
18. Motor
19. Variac

Fig.1. Schematic diagram of the experimental set-up Once the flow is stabilized and the stagnation condition is achieved, readings for

inlet and outlet air temperatures, plate temperatures, pressure drop across the duct and the orifice and solar insolation is recorded. Photograph of the experimental set-up is shown in Fig. 2

Fig.2. Photograph of the experimental set-up

The thermocouples were connected to a digital voltmeter indicating their output. The pressure drop across the orifice was measured with a U-tube manometer and along the duct was measured using multi-tube manometer having least count of 0.001 mm of H2O. Pyranometer was used to measure the intensity of solar radiation and ambient temperature at different time intervals. The range of operating parameters is shown in Table. 1.

Table 1. Range of operating parameters

S. No.	Name of parameter	Symbolic representation	Range of operating parameter
1.	Reynolds number	Re	2500-12500
2.	Relative roughness pitch	p/e	8-15
3.	Relative roughness height	e/D_h	0.018-0.045
4.	Ambient temperature	T_∞	(24-44) ˚C
5.	Solar insolation	I	(720-960) W/m^2

3. Data Reduction

The recorded data from experimentation for plate and air temperatures under steady state conditions at a varying mass flow rate and heat flux was used to calculate the heat transfer from the absorber plate to the under flowing air. Using the pressure drop across the orifice plate, the prevailing mass flow rate across the duct is:

$$m = C_d \, A_o \left[\frac{2 \rho_a \Delta P_o \sin\theta}{1-\beta^4} \right]^{0.5} \quad (1)$$

Heat lost by the collector = Heat gained by the under flowing air

$$\text{i.e. } hA_p \left(T_{pm} - T_{fm}\right) = mC_p \left(T_o - T_i\right) \quad (2)$$

$$\text{i.e. } h = \frac{mC_p \left(T_o - T_i\right)}{A_p \left(T_{pm} - T_{fm}\right)} \quad (3)$$

Nusselts number is determined using heat convective heat transfer co-efficient as:

$$Nu = \frac{hD_h}{K} \quad (5)$$

The friction factor was determined for the test length 1500 mm using Darcy Weisbach equation as:

$$f = \frac{(\Delta P_d) D_h}{2\rho L V^2} \quad (6)$$

The uncertainty prevailing in the measurement of various parameters has been calculated following a simple procedure suggested by Klein and McClintock [22], the values of uncertainty involved in the measurement of Nusselts number and friction factor were found to be □3.28 % and □4.16 % respectively.

4. Validation

The experimental values of Nusselts number and friction factor for one side concave dimple roughened duct have been compared with those of a similar duct model adopted by Saini and Verma [23].

The Nusselts number and friction factor for one The value for Nusselts number and friction

factor for one side dimple roughened duct was

side dimple roughened duct is given by the eq.

found to compare well with the values so no. 9 and 10.

obtained from the correlations suggested by

1.15 □ e □ 0.0333

Saini and Verma. The mean deviation between

□ p □

Nu1r □ 5.2 □10 □4 1.27

(Re) □ □ □ □ the estimated and the experimental value was

□ e □ □ Dh □

□ □ □ p □ □2□□ found to be following and the same has been

□□□ exp(□2.12)□ log □ □ □

□ shown in Fig.7 and 8:

□ □ □ e □ □ □ (9)

□ □

□ □ □ e □ □2□□

□□□ exp(□1.30)□ log □ □ □

□ □ □3.7% (Nusselts number)

D

□ □ □ □ □ □

□ □ h □ □ □ □ 4.5% (Friction factor)

f1r □ 0.642 Re □0.423 □ p / e □ □0.465 □ □e / Dh □□0.0214 (10)

□ 2 □

□ □ exp □0.054 □□log □ p / e□□

□

□ □

□ □□□ exp □0.840 □□log □e / Dh □ □2 □□□

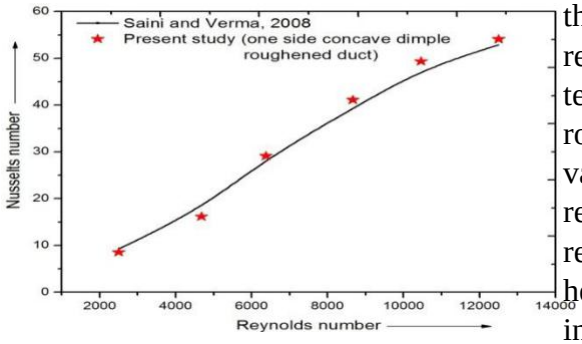

Fig. 7. Comparison of estimated and experimental values of 'Nu' for one side roughened duct

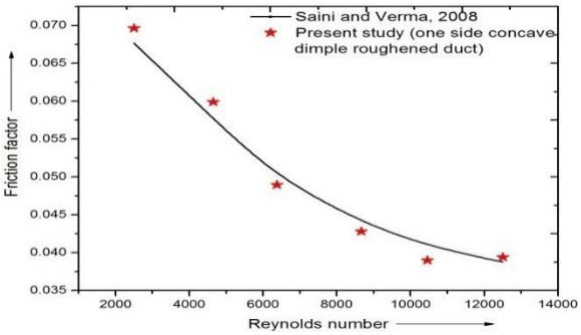

Fig. 8. Comparison of estimated and experimental values of 'f' for three sides roughened duct Based on the above comparison, reasonably good agreement between the experimental and estimated values of Nusselts number and friction factor guarantees the exactness of the information being gathered from this test setup.

5. Results and Discussions

The effects of dimple shape roughness element and the variation in the roughness parameter on heat transfer and fluid flow characteristics has been investigated and discussed. The values of the Nusselts number and friction factor for the three sides roughened ducts as a function of Reynolds number have been compared to those of one side roughened duct under identical experimental conditions.

5.1 Nusselts number

The augmentation in Nusselts number achieved as a result of providing artificial roughness in the form of concave dimple shape on the three sides roughened duct over one side roughened duct with an increasing Reynolds number for varying relative roughness pitch (p/e) and relative roughness height (e/Dh) is shown in Fig. 9 and Fig. 10.

Fig. 9 depicts that with an increase in p/e ratio, the Nusselts number increases, but only up to a relative roughness pitch of 12 beyond which it tends to decrease with an increase in relative roughness pitch. The maximum and minimum values of Nusselts number is obtained at the relative roughness pitch value of 12 and 8 respectively at a constant relative roughness height of 0.036 for the range of parameters investigated.

Fig. 10 shows the effect of relative roughness height on Nusselts number. The maximum heat transfer rate is achieved at the relative roughness height of 0.036.

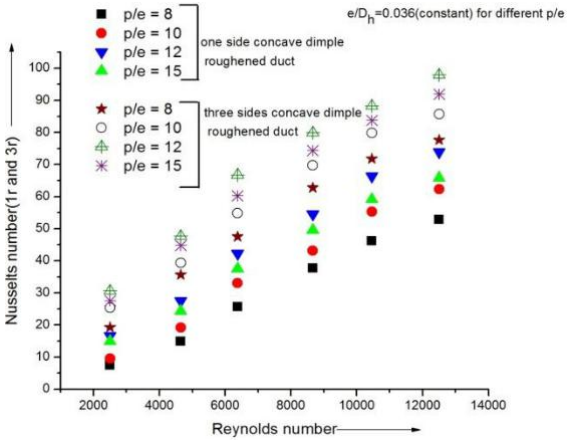

Fig.9. Effect of relative roughness pitch on 'Nu' for one and three sides roughened duct

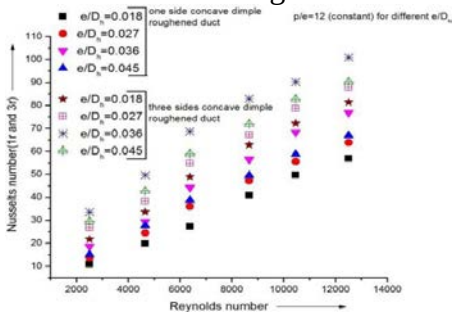

Fig.10. Effect of relative roughness height on 'Nu' for one and three sides roughened duct

5.2 Friction Factor

Artificially roughened SAHs are often characterized by the rise in pressure drop across the roughened duct, which results in an increment of friction co-efficient leading to a higher pumping power requirement. Numerous researchers have worked on different roughness geometry, trying to optimize the geometrical parameter to obtain a minimum rise in friction co-efficient. The effect of relative roughness pitch (p/e) and relative roughness height (e/Dh) on the friction factor with increasing Reynolds number is shown in Fig. 11 and 12 respectively.

Fig. 11 shows the variation in friction factor of three sides over one side roughened duct with Reynolds number with an increasing relative roughness pitch ratio. As the Reynolds number increases, the friction factor decreases monotonously. The three sides roughened duct requires more pumping power than one side roughened duct. For both the roughened ducts, friction factor decreases with increasing relative roughness pitch. The maximum and minimum friction factor for both three sides and one side roughened ducts is obtained at the relative roughness pitch values of 8 and 15 respectively.

Fig. 12 shows the variation in friction factor with Reynolds number with increasing relative roughness height ratio. It can be concluded that as the Reynolds number increases, the friction factor decreases with decreasing relative roughness pitch. Efforts should be made to optimize the geometrical parameter to achieve maximum heat transfer rate at a minimum rise in the co-efficient of friction. The maximum and minimum friction factor for both three sides and one side roughened duct is obtained at relative roughness height ratio of 0.045 and 0.018 respectively.

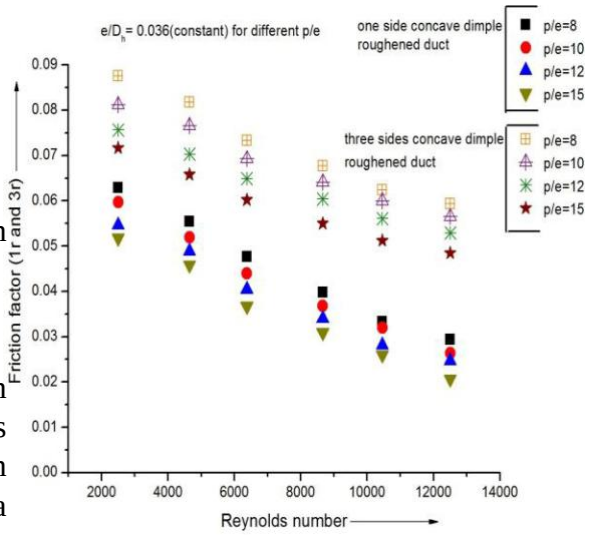

Fig.11. Effect of relative roughness pitch on 'f' for one and three sides roughened duct

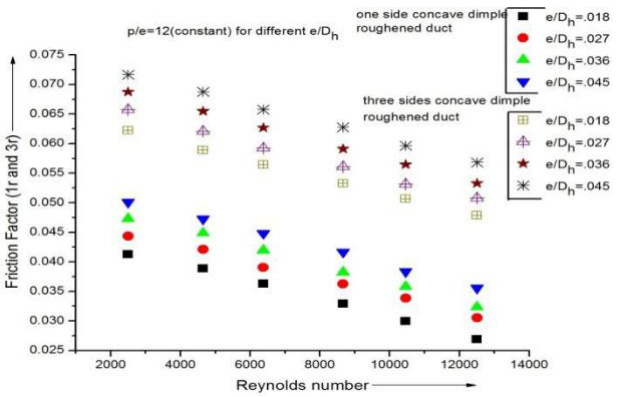

Fig.12. Effect of relative roughness height on 'f' for one and three sides roughened duct

6 Conclusions

Roughness geometry in the form of concave dimple resulted in an appreciable augmentation of heat transfer with an allowable rise in friction characteristics; following conclusions can be drawn:

- The maximum values of Nusselts number were obtained at relative roughness pitch of 12 and relative roughness height of 0.036.
- The augmentation in the Nusselts number of three sides roughened duct over one side roughened duct for varying relative roughness pitch in the range of parameters investigated was found to be 25-86%.
- The enhancement in the Nusselts number of three sides roughened duct over one side roughened duct for varying relative roughness height in the range of parameters investigated was found to be 21-81%.
- The maximum values of friction factor were obtained at relative roughness pitch of 8 and relative roughness height of 0.045.
- The augmentation in friction factor of three sides roughened duct over one side roughened duct for varying relative roughness pitch and relative roughness height was found to be respectively as 11-34% and 15-41% in the range of parameters investigated.
- The average enhancement in the Nusselts number for three sides roughened duct over one side roughened duct for varying relative roughness pitch and relative roughness height was respectively found to be as 59% and 48% in the range of parameters investigated

References

1. Hsieh, J.S., Solar energy engineering. New Jersey: Prentice Hall; 1986.

2. Sharma, S.K., Kalamkar, V.R., Thermo-hydraulic performance analysis of solar air heaters having artificial roughness–A review Renewable and Sustainable Energy Reviews 41 (2015) 413–435.

3. Duffie, J.A., Beckman, W.A., Solar engineering thermal processes, 2nd ed. New York: John Wiley; 1991.

4. Sukhatme, S.P., Solar energy: Principles of thermal collection and storage, 9th Ed. New Delhi: Tata McGraw-Hill; 2003.

5. Dippreyy, D.F., Sabersky, R.H., Heat and momentum transfer in smooth and rough tubes at various Prandtl numbers. Int J Heat Mass Transf 1963; 6:329–53.

6. Webb, R.L., Eckort, E.R.G., Goldstein, K.J., Heat transfer and friction in tubes with repeated rib roughness. Int J Heat Mass Transf 1971; 14:601–17.

7. Firth, R.J., Meyer, L., A comparison of the heat transfer and friction factor performance of four different types of artificially roughened surface. Int J Heat Mass Transf 1983; 26(2):175–83.

8. Nguyen, T.M., Khodadadi, J.M., Vlachos, N.S., Laminar flow and conjugate heat transfer in rib roughened tubes. Numer Heat Transf Part A: Appl: Int J Comput Methodol 1989; 15:165–79.

9. Prasad, B.N., Saini, J.S., Effect of artificial roughness on heat transfer and friction factor in a solar air heater. Sol Energy 1988; 6:555–60.

10. Varun, Saini, R.P., Singal, S.K., A review of roughness geometry used in solar air heaters. Sol Energy 2007; 81:1340–50.

11. Ahn, S.W., The effect of roughness types on friction factor and heat transfer in roughened rectangular duct. Int Commun Heat Mass Transf 2001; 28:933–42.

12. Singh, A.P., Varun, Siddhartha, Effect of artificial roughness on heat transfer and friction characteristics having multiple arc shaped roughness element on the absorber plate. Sol Energy 2014; 105: 479–493.

13. Alam, T. and Kim, M.H., A critical review

on artificial roughness provided in rectangular solar air. Renewable and Sustainable Energy Reviews 69 (2017) 387–400.

14. Hans, V.S., Saini, R.P. and. Saini, J.S. Performance of artificially roughened solar air heater-A review, Renewable and Sustainable Energy Reviews, 13, 2009, 1854-1869.

15. Gupta, D., Solanki, S.C., Saini, J.S.,

Heat and fluid flow in rectangular solar air heater ducts having transverse rib roughness on absorber plates. Sol Energy 1993; 51:31–37.

16. Gupta, D., Solanki, S.C., Saini, J.S., Thermohydraulic performance of solar air heaters with roughened absorber plates. Sol Energy 1997; 61:33–42.

17. Momin, A.M.E., Saini, J.S., Solanki, S.C., 2002. Heat transfer and friction in solar air heater duct with v-shaped rib

roughness on absorber plate. International Journal of Heat Mass Transfer 45, 3383–3396.

18. Varun, Saini, R.P., Singal, S.K., Investigation of thermal performance of solar air heater having roughness elements as a combination of inclined and transverse ribs on the absorber plate. Renew Energy 2008; 33:1398–405.

19. Prasad, B.N., Behura, A.K. and Prasad, L., Fluid flow and heat transfer analysis for heat transfer enhancement in three sided artificially roughened solar air heater. Sol. Energy 105, 2014, 27–35.

20. Behura, A.K., Prasad, L. and Prasad, B.N., Heat transfer, friction factor and thermal performance of three sides artificially roughened solar air heaters. Solar Energy 130 (2016) 46–59.

21. ASHRAE, Standard, 93–97, 1977. Method of testing to determine the thermal performance of solar air heater.

American society for heating, refrigeration and air conditioning engineering, New York, pp. 1–34.

22. Kline, S.J., McClintock FA. Describing uncertainties in single sample experiments. Mechanical Engineering 1953; 75: 3-8.

23. Saini, R.P., Verma, J., Heat transfer and friction factor correlations for a duct having dimple-shape artificial roughness for solar air heaters. Energy 2008; 33:1277–87.